REPORT DOCUMENTATION PAGE

Form Approved
OMB No. 0704-0188

1. AGENCY USE ONLY (*Leave Blank*)	2. REPORT DATE	3. REPORT TYPE AND DATES COVERED
	4/11/97	Interim Progress Report 3/1/96 3/31/97

4. TITLE AND SUBTITLE
Hydrodynamic Interaction Between Olfactory Antennae and Odor Plumes

5. FUNDING NUMBERS
N00014-96-1-0594

6. AUTHORS
Koehl, Mimi, A. R.

7. PERFORMING ORGANIZATION NAME(S) AND ADDRESS(ES)
Sponsored Project Office
336 Sproul Hall
University of California
Berkeley, CA 94720-5940

8. PERFORMING ORGANIZATION REPORT NUMBER
N/A

9. SPONSORING / MONITORING AGENCY NAME(S) AND ADDRESS(ES)
Dr. Eric Eisenstadt
Office of Naval Research
800 North Quincy St
Arlington, VA 22217-5660

10. SPONSORING / MONITORING AGENCY REPORT NUMBER
N/A

11. SUPPLEMENTARY NOTES
N/A

12a. DISTRIBUTION / AVAILABILITY STATEMENT
Unlimited

12b. DISTRIBUTION CODE
N/A

13. ABSTRACT (*Maximum 200 words*)

We have been studying the hydrodynamic performance of olfactory appendages of marine animals, both to elucidate how they filter chemical cues from the environment, and to gain insights for the design of man-made chemical sensors. The interaction of an appendage with ambient odor plumes and the small-scale velocity field near the appendage's surface determines the rates and locations at which molecules are encountered. Our objectives are to determine how the flow microenvironments and odorant encounter of these appendages are affected by 1) the presence and arrangement of sensory hairs, and 2) the flicking of the appendages in realistic odor plumes. During year one of this grant we have undertaken morphometric and kinematic analysis of olfactory antennules of stomatopods, completed such an analysis for lobsters, conducted experiments with dynamically-scaled physical models of lobster antennules to determine the effects of speed and orientation of flow near sensory hairs, and begun measuring water flow and mass transport in the habitats of nudibranchs whose olfactory rhinophores we are studying.

14. SUBJECT TERMS: waves, low Reynolds number, olfaction, antennule, rhinophore, chemosensation, boundary layer, plume dispersion	15. NUMBER OF PAGES 9
	16. PRICE CODE

17. SECURITY CLASSIFICATION OF REPORT	18. SECURITY CLASSIFICATION OF THIS PAGE	19. SECURITY CLASSIFICATION OF ABSTRACT	20. LIMITATION OF ABSTRACT
Unclassified	Unclassified	Unclassified	UL

NSN 7540-01-280-5500

Standard Form 298 (Rev. 2-89)
Prescribed by ANSI Std. Z39-1
298-102

O.N.R. GRANT #N00014-96-1-0594, PROGRESS REPORT: 3/1/96 - 3/31/97

"Hydrodynamic Interaction Between Olfactory Antennae and Odor Plumes"

M.A.R. Koehl, Department of Integrative Biology, University of California, Berkeley, CA 94720-3140

Goals

We have been studying the hydrodynamic performance of olfactory appendages of marine animals, both to elucidate how they filter chemical cues from the environment, and to gain insights for the design of man-made chemical sensors.

Objectives

Some olfactory appendages are simple rods while others have sensory hairs in various arrangements. The interaction of an appendage with ambient odor plumes and the small-scale velocity field near the appendage's surface determines the rates and locations at which molecules encounter the surface. Our objectives are to determine how the flow microenvironments and odorant encounter of these appendages is affected by 1) the presence and arrangement of sensory hairs, and 2) the flicking of the appendages in realistic odor plumes.

Approach

We are comparing the flow microenvironment and molecule capture by olfactory appendages bearing sparse, dense, or no hairs (crustacean antennules, opisthobranch rhinophores) We are using dynamically-scaled physical models to study the effects of appendage morphology and kinematics on the flow fields near sensor surfaces , and we plan to conduct flume experiments to quantify how the information in odor plumes is altered by the physical structure and the motions of various designs of olfactory appendages.. We are conducting morphometric and kinematic analyses of olfactory appendages and field measurements of flow to ensure the relevance of these model and flume experiments to real biosensors in coastal environments.

Tasks Completed and Results During Year One

During the first year of this grant, we have focused on the olfactory antennules of stomatopods (various species that vibrate antennules bearing a simple, sparse array of sensory hairs), lobsters (*Panulirus argus*, which flick antennules bearing a complex, dense array of guard and sensory hairs), and opisthobranch mollusks (*Phestilla sibogae* , which capture odors on ciliated, non-flicking rhinophores).

Stomatopods:

We have been conducting morphometric, kinematic, and field investigations of a variety of species of stomatopods in order to select the species for more intensive study. Our light micrographs and SEM's of antennules from 15 species revealed diverse variations of the same basic structure (Fig. 1). Stomatopod antennules have three branches ("flagella"); three olfactory

hairs ("aesthetascs") per segment are borne on the distal end of the middle flagellum. The size and shape of the flagella, and the size, shape, and orientation of the aesthetascs vary between species. We have focused on *Gonodactylus mutatis* to explore the scaling of olfactory structures as the animals grow, and have begun morphometric analysis of 40 animals representing an order of magnitude range in body length.

We have also been conducting high-speed 3-D video studies of antennule motions of three species in the lab to work out the techniques for kinematic analysis. Antennulation involves small (amplitude of flagella tips = 1 to 2 mm), rapid (maximum velocity = 0.14 m/s) vibrations of an antennule. The antennule vibrations (frequencies of 1 to 10 Hz) can be in any plane, and are interrupted by pauses. The Reynolds numbers (Re = ratio of inertial to viscous forces determining the water flow) of the aesthetascs range from 0.5 to 4; this is a Re range in which water can penetrate rows of hairs and in which flow is very sensitive to hair spacing (Koehl, 1996a; 1996b).

We have surveyed stomatopods at a variety of field sites in California and Hawaii, and have chosen to focus on two Hawaiian species (*G. mutatis*, *Pseudosquilla ciliata*) that are abundant, easy to collect, and occur in shallow habitats where ambient water flow can be readily measured. We have established field sites near Coconut Island, HI, and have begun videotaping animals in the field.

Lobsters:

We have chosen to focus on the antennules of the Florida spiny lobster, *P. argus,* whose neurobiology has been extensively studied. Our morphometric analysis of their antennules (based on SEM and light microscopy) and our kinematic analysis of their antennule flicking (based on high-speed video) is now complete. The animals flick the aesthetasc-bearing lateral branch of their antennules down quickly and up slowly (Fig. 2,A), with the aesthetascs oriented at an angle of 32° relative to the plane of motion. We found that aesthetasc number, size, spacing, orientation, and speed during flicking does not change as the lobsters grow, hence Re is maintained at a value of 1 to 2 across a range of body sizes (Fig. 2).

We have built dynamically-scaled physical models of *P. argus* antennules (based on our morphometric and kinematic data) to enable us to measure detailed flow velocity fields around them. We are using these models have to quantify the consequences of orientation, Reynolds number, and morphology on the penetration of fluid into the hair arrays (Fig. 3). Such experiments have shown that fluid to moves through the aesthetasc array at the orientation used by the lobsters (A & B), but bypasses it if the hairs point directly into or away from the flow.

Our kinematic analysis of antennule flicking by real *P. argus* antennules on model lobsters in "odor" (fluorescein and dopamine in sea water) plumes in a flume is nearly complete. IVEC probes measuring the rate of dopamine arrival within the aesthetasc array on these antennules show that flicking seems to enhance the probability of the sensors encountering dye filaments, but that

the odor molecules do not arrive at the sensor until after both the downstroke and the upstroke of the flick are completed (Moore, Best, Schneider, Gorski, and Koehl, 1996). (Before we did this work, it was assumed that the smell penetrated the aesthetasc array during the downstroke and neurobiological experiments were conducted accordingly.) Our results are consistent with predictions made by mathematical modeling of another species of lobster, *Homarus americanus*, by my collaborator at UC Davis, Angela Cheer (Cheer, Ogami, and Koehl, in prep.). We plan to repeat these experiments in collaboration with Koseff and Crimaldi in the big Stanford flume and wave tank (where we can do more realistic simulation of turbulent mixing of odorants than we were able to do in my little flume at Berkeley).

Opisthobranch-Mollusks:

We are studying the rhinophores of *P. sibogae* in Hawaii in collaboration with Budko and Hadfield, who have been mapping their olfactory receptors. Thus far my work has focused on field studies of water flow around and through the coral (*Porites compressa*) reef habitats of *P. sibogae*. in Kaneohe Bay, HI. We are using an acoustic doppler velocimeter to measure water velocity profiles above patch reefs, and we are analyzing video records of the transport and dispersion of dye to quantify advection and turbulent mixing at these sites. We are finding that the flow is dominated by wave action, that advection is slow but mixing via shear dispersion is high, and that water is slowly pumped through the infrastructure of the reefs, moving in at the reef front and back and out through the top. Such field data will provide the information necessary to set up realistic lab wave-tank experiments to investigate the effects of rhinophore morphology on the information in odor plumes.

We have also begun to work out the technical details to study the small-scale flow produced by the cilia beating on the surfaces of *P. sibogae* rhinophores.

Summary of Accomplishments During Year One (Our New Discoveries)

Our studies of stomatopod and lobster antennules are revealing that the olfactory hairs on these appendages from a variety of species and sizes of animals operate at Re's of order one. This Re represents an intriguing flow regime in which fluid can move through rather than around arrays of hairs, but in which the arrangement and orientation of the hairs can have a big effect on flow. Our mathematical models and pilot flume experiments suggest that odorants are captured during the upstroke or after a flick has been completed, rather than during the downstroke, as had previously been believed.

Our measurements of water flow in shallow coastal field sites are revealing that advection is slow and shear dispersion is high in the oscillatory flow driven by waves, hence unidirectional odor plume studies, as have been done in flumes in the past, are inappropriate for assessing the performance of olfactory sensors in such habitats.

Publications During Year One

(Papers published this year reporting research supported by my previous ONR grant on olfactory appendages, #N00014-90-J-137)

Koehl, M. A. R. (1996a) Small-Scale fluid dynamics of olfactory antennae. Mar. Fresh. Behav. Physiol. 27: 127-141.

Koehl, M. A. R. (1996b) When does morphology matter? Ann. Rev. Ecol. Syst. 27: 501-542.

Moore, P.A., B. Best, R. Schneider, L. Gorski, and M.A.R. Koehl (1996) Olfactory sampling in lobsters: Chemical dynamics during flicking and recovery in the Maine and spiny lobsters (abstract). Chem. Senses 21: 645.

Invited Talks (by M. Koehl) During Year One Based on ONR-Supported Research

Department of Zoology, University of Wisconsin, Madison

Biofluid Dynamics Symposium, Special Year in Mathematical Biology, University of Utah

Gordon Conference on Theoretical Biology and Biomathematics (Thursday night speaker)

Center for Theoretical Dynamics, University of California, Davis

Department of Biology, University of Virginia

Statistics: EEO and Minority Support

Postdocs: This grant is supporting one female postdoc: Kristina Mead.

Graduate Students: Although no graduate student stipends were paid from this grant, three graduate students participated in model experiments measuring flow fields around hair-bearing appendages at low and intermediate Reynolds numbers: Jason Jed, Michael McCay, and Marlene Martinez (minority female)..

Undergraduates: Two undergraduates conducted supervised research projects that were part of this ONR study: Tzu-lung Hu measured flow around dynamically-scaled physical models of *P. argus* antennules, and Lydell Gorski quantified the kinematics of *P. argus* antennules in pilot experiments for flume studies of the effects of flicking. In addition, a recent graduate volunteering in the lab, Michael O'Donnell, has been working with Dr. Mead on the high-speed videotaping of stomatopod antennules.

FIGURE LEGENDS

Figure 1. Scanning electron micrographs (SEM's) of the antennules of stomatopods, illustrating examples of diverse antennule shapes and sizes, and aesthetasc (olfactory hair) sizes and orientations (scale bar in μm's below each photograph). A. SEM of the antennule of a *Gonodactylus viridis*, showing the three flagella of the antennule. The middle flagella bears the aesthetascs. B. Higher magnification SEM of the aesthetascs on the middle flagella of the antennule of a *Gonodactylus mutatis*. C. SEM of the long, slim antennule of a *Haptosquilla stoliura*. D. SEM of the short, wide antennule of a *Gonodactyllelus annularis*.

Figure 2. Kinematic measurements from high-speed video analysis of the flicking of the lateral antennules of spiny lobsters (*Panulirus argus*). A. Example of the velocity of the lateral branch of an antennule during a flick, plotted as a function of time. Velocity of the antennule during the downstroke ("Flick") is designated as positive, and velocity of the antennule during the upstroke ("Recovery") is designated as negative. The solid line indicates the velocity of the tip of the antennule; the dashed line indicates the velocity of the position on the antennule of the midpoint of the tuft of aesthetascs, which is on the distal portion of the antennule. Note that the downstroke is faster and of shorter duration than the upstroke. B. Angle of attack (angle between the long axis of the lateral branch of the antennule and the direction of water motion relative to it) of the antennule plotted as a function of lobster size (carapace length). The mean angle of each flick downstroke and upstroke was calculated from all frames digitized; 15 flicks per animal were analyzed. Each point in this graph represents the mean of those 15 flicks for an individual lobster, and the error bars indicate one standard deviation. Squares are values for the downstrokes and x's are values for the upstrokes. C. Speed of the midpoint of the aesthetasc tuft of the lateral branch of an antennule, plotted as a function of lobster carapace length. Open circles represent the mean of the maximum speeds achieved during the downstrokes of 15 flicks, x's represent the mean of the mean downstroke speeds of those 15 flicks, and black squares represent the mean of the mean speeds of the upstrokes of those 15 flicks. Error bars represent one standard deviation. D. Reynolds numbers (Re's) of the aesthetascs of the lateral branches of the antennules, plotted as a function of lobster carapace length. Each point represents the aesthetasc Re of an individual animal calculated using the mean diameter of the aesthetascs on its antennule (measured on SEM's). Open circles represent the Re's attained at the time of maximum velocity during the downstroke, x's represent the mean Re during the downstroke, and black squares represent the mean Re during the upstroke. Note that the Re of the aesthetascs is maintained as the animals grow, and that the maximum Re of the upstroke is 2, while that of the downstroke is 0.5.

Figure 3. Examples of velocity fields measured around dynamically-scaled physical models of the lateral branch of the antennule of a *Panulirus argus*. The model is seen in cross-section and the digitized paths of neutrally-buoyant flow markers are shown as dots. The model was moved at an angle of attack of 90^{o} through stationary fluid (direction indicated by large arrow), but the diagrams indicate the fluid velocity *relative to* the model. Small arrows indicate the direction of fluid motion relative to the model, while the distance between the dots along a streamline indicates the speed of the flow (velocity scale bars, which are different for each diagram, are given in antennule diameters per second). A. Downstroke of the antennule, with aesthetascs at an angle of 32^{o} relative to the oncoming flow; Re = 2. B. Upstroke of the antennule, with aesthetascs at an angle of 148^{o} relative to the oncoming flow, Re = 0.5. The volume flow rate through the aesthetasc array is greater during the downstroke than during the upstroke. C. Downstroke of the antennule, with aesthetascs at an angle of 0^{o} relative to the oncoming flow; Re = 2. B. Upstroke of the antennule, with aesthetascs at an angle of 180^{o} relative to the oncoming flow, Re = 0.5. Fluid to moves through the aesthetasc array at the orientation used by the lobsters (A & B), but bypasses it if the hairs point directly into or away from the flow (C & D).

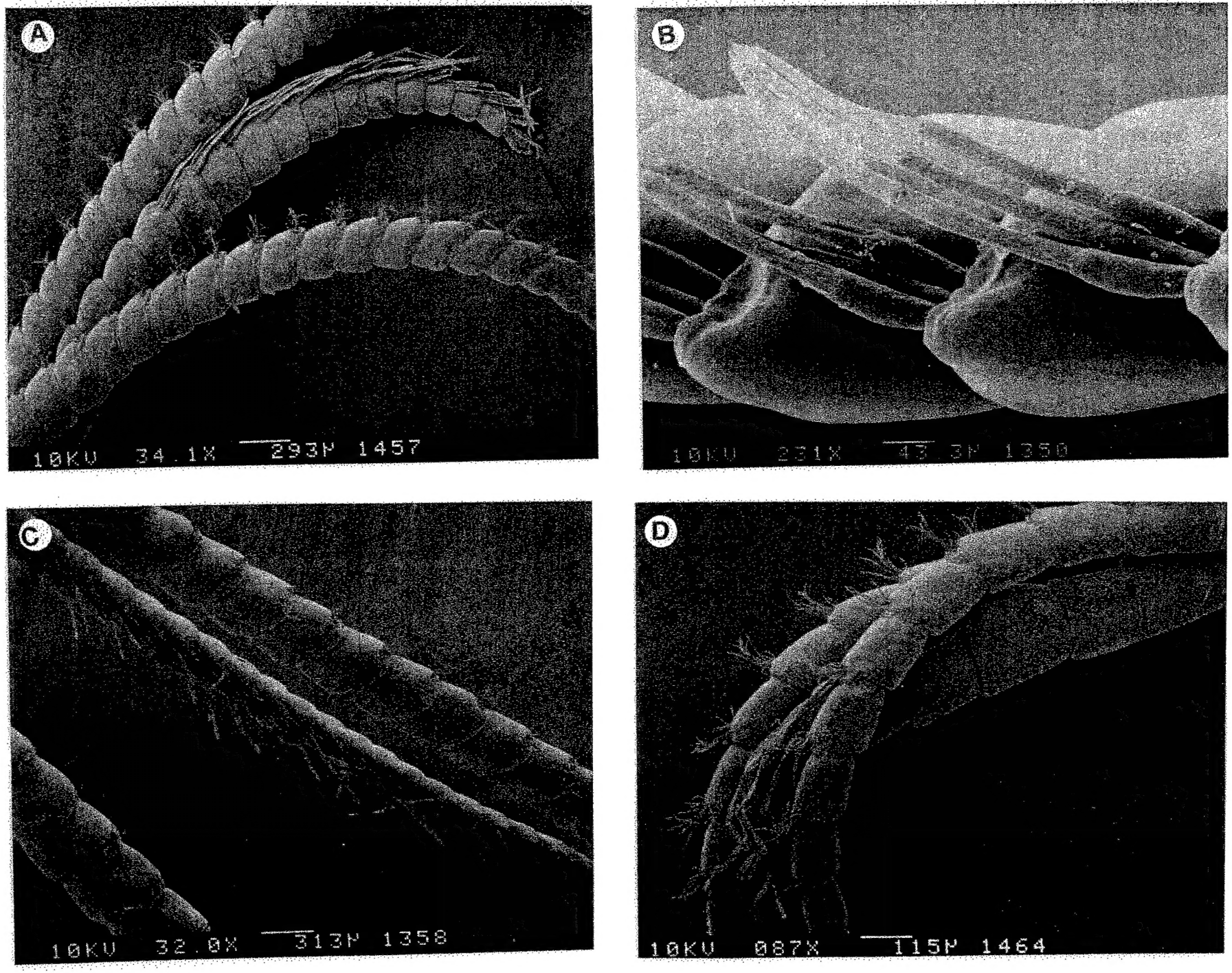
A
10KU 34.1X 293µ 1457
B
10KU 231X 43 3µ 1350
C
10KU 32.0X 313µ 1358
D
10KU 087X 115µ 1464

Fig. 1

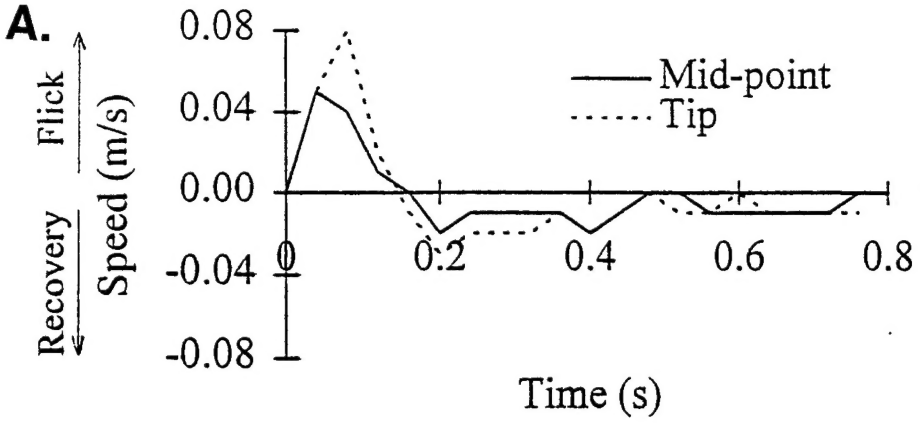
A.
Flick
Recovery
Speed (m/s)
0.08
0.04
0.00
-0.04
-0.08
0
0.2
0.4
0.6
0.8
Mid-point
Tip
Time (s)

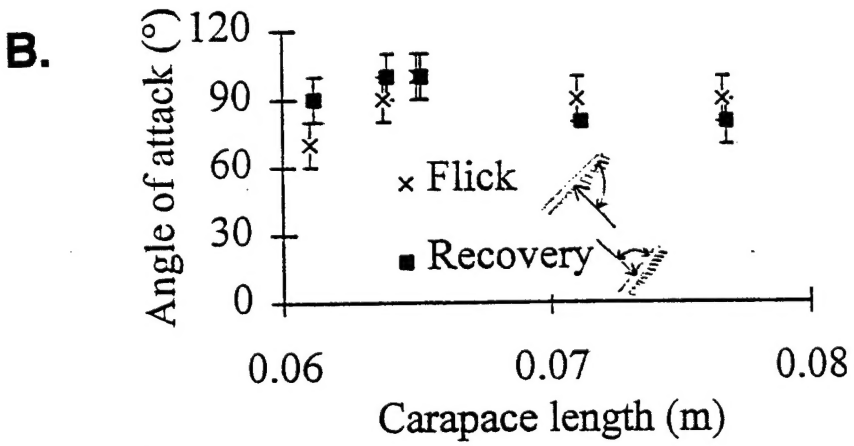
B.
Angle of attack (°)
120
90
60
30
0
× Flick
■ Recovery
0.06
0.07
0.08
Carapace length (m)

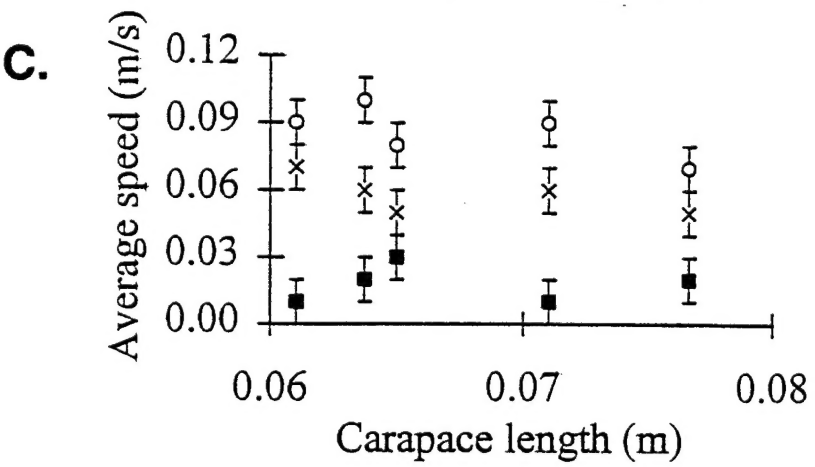
C.
Average speed (m/s)
0.12
0.09
0.06
0.03
0.00
0.06
0.07
0.08
Carapace length (m)

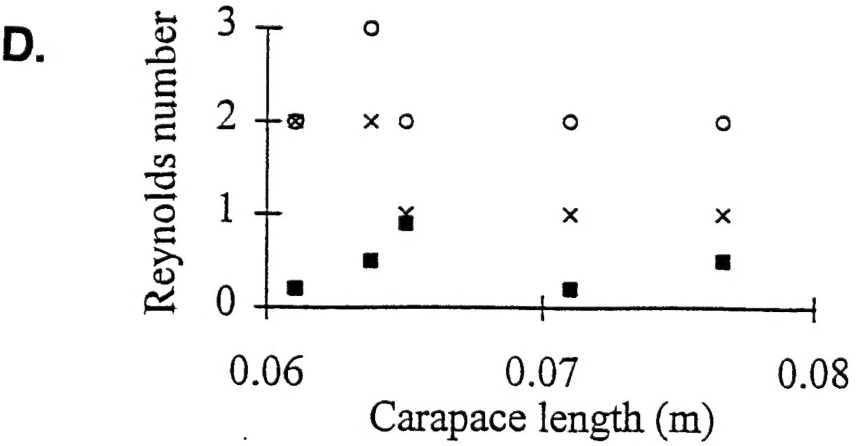
D.
Reynolds number
3
2
1
0
0.06
0.07
0.08
Carapace length (m)

Fig. 3

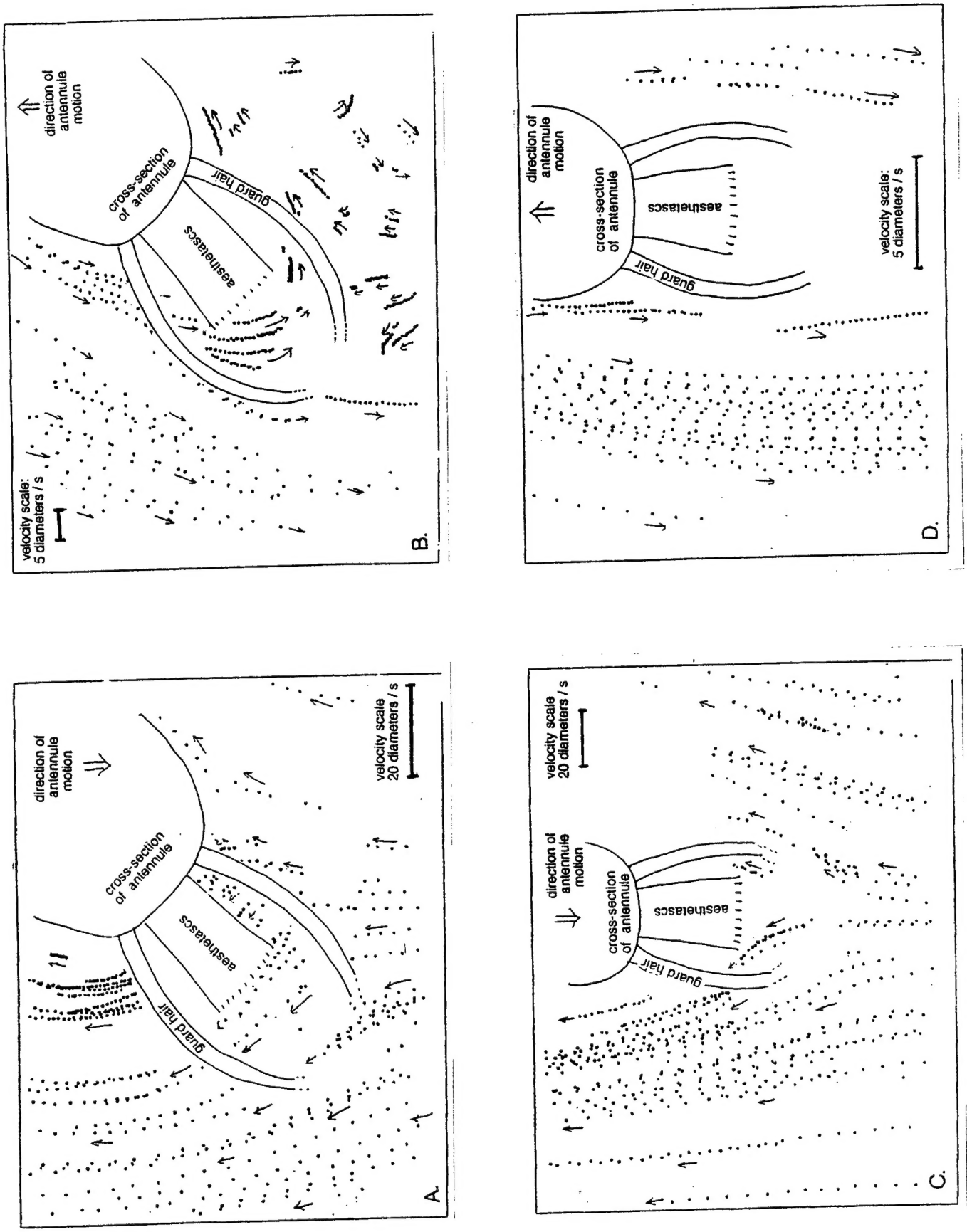
direction of antennule motion
cross-section of antennule
guard hair
aesthetascs
velocity scale: 5 diameters / s
B.
direction of antennule motion
cross-section of antennule
aesthetascs
guard hair
velocity scale: 5 diameters / s
D.
direction of antennule motion
cross-section of antennule
guard hair
aesthetascs
velocity scale 20 diameters / s
A.
velocity scale 20 diameters / s
direction of antennule motion
cross-section of antennule
aesthetascs
guard hair
C.